Carbohydrate Polymers **6** (1986) 121–143

The Relationship of the Crystal Structure of Amylose Polymorphs to the Structure of the Starch Granule

D. L. Wild* and J. M. V. Blanshard

Department of Applied Biochemistry and Food Science, Nottingham University
School of Agriculture, Sutton Bonington, Loughborough, Leicestershire,
LE12 5RD, UK

(Received: 30 August 1985)

SUMMARY

A detailed comparison has been made between wide-angle X-ray powder diffraction patterns obtained from A and B type starch granules and simulated patterns calculated from the published crystal structures of A and B amyloses.

Although the simulated patterns reproduced the main features of the experimental ones, a number of discrepancies were apparent, mainly at interplanar spacings of > 0·5 nm. These did not appear to be simply due to the packing sense of the amylose double helices in the unit cell. A number of peaks in the simulated patterns for B amylose appeared sensitive to the positions of the water molecules in the model structure.

Preliminary neutron powder diffraction data from B type starch granules in H_2O and D_2O have also been measured and compared with profiles calculated from the B amylose structure.

INTRODUCTION

The starch granule is a semi-crystalline polymer spherulite composed of the linear poly-α-1,4-glucan amylose and the branched polyglucan, amylopectin. When examined by wide-angle X-ray powder diffrac-

---

*Present address: European Molecular Biology Laboratory, Grenoble Outstation, c/o ILL, BP 156X, 38042 Grenoble Cedex, France.

tion, starch granules give distinctive scattering patterns of three main types: 'A' patterns, characteristic of cereal starches; 'B' patterns, characteristic of tuber, fruit and stem starches; and 'C' patterns, characteristic of bean starches, which have been interpreted as an intermediate between A and B (Katz & Van Itallie, 1930; Charbonnière *et al.*, 1968).

A variety of evidence suggests that the branched amylopectin is responsible for the crystalline regions of the granules, with the linear amylose being present in the amorphous regions, a suggestion originally mae by Meyer (1942). This view is supported by a number of observations. For example, if the amylose is dissolved out of the granule, the crystalline structure is maintained (Montgomery & Senti, 1958), while waxy maize starch, which contains no amylose, also exhibits an 'A' type X-ray diffraction pattern similar to normal maize starch (Charbonnière *et al.*, 1968). Further, the behaviour of the granules in polarized light suggests that the polymer chains are arranged radially (French, 1972).

A number of studies have attempted to elucidate the crystallographic structure of the polyglucan chains in the starch granule. The first attempt was made by Kreger (1951), who was able to obtain an oriented fibre-like X-ray diffraction pattern from part of a large single B type starch granule by the use of a specially designed microcamera. Further progress came with the use of artificial fibres of 'A' and 'B' amylose. A major step forward was taken by Wu & Sarko (1978*a,b*), who, on the basis of a combination of X-ray diffraction data obtained from amylose fibres, and computer modelling techniques, proposed crystal structures for A and B amylose, based on two right-handed, parallel-stranded, six-fold double helices packed in an anti-parallel fashion in the unit cell. The two polymorphs possess the same double helical structure but exhibit different crystalline packing (Fig. 1). However, a structure based on a left-handed six-fold helix has also been proposed for B starch by Brant (1976) and Cleven *et al.* (1978). Wu & Sarko (1978*a,b*) also proposed that, in the 'B' structure, 36 water molecules are located in a channel in the centre of a hexagon of double helices (Fig. 1(b)), whilst in the 'A' structure eight water molecules are distributed equally in spaces between the helices (Fig. 1(a)). The similarity between the values of the interplanar spacings (*d*-spacings) obtained from A and B amylose fibres, and those obtained from native starch granules (Sarko & Wu, 1978), has led to

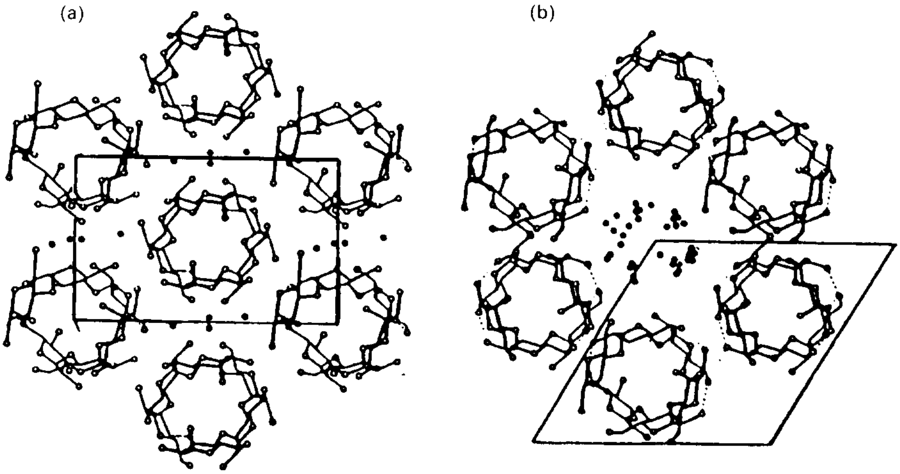

Fig. 1. The unit cells and helix packing in the crystal structures of (a) A and (b) B amyloses. The positions of the water molecules are marked by black dots. From Wu & Sarko (1978*b*). Reproduced with permission.

the assumption that the amylopectin molecules responsible for the crystallinity of the starch granule have the same crystalline structure as the artificial fibres of A and B amylose. However, as French (1984) has pointed out, the proposed anti-parallel packing of the double helices seems problematic on biosynthetic grounds and, in fact, there is still some uncertainty about this particular aspect of the model proposed by Wu & Sarko. The two-dimensional crystallographic *R*-factor for the 'best' model for B amylose (with anti-parallel packing of the double helices) was 6·5%, whilst the value for the equivalent model with parallel packing was 13·5% (Wu & Sarko, 1978*a*). Sarko (pers. comm.) has pointed out that, as the analysis stands, the anti-parallel packing of the double helices is still not clearly determined.

There is also some uncertainty about the precise positions of the water molecules shown in Fig. 1. Wu & Sarko (1978*a*) refer to the somewhat indeterminate character of the water molecules in B amylose, and the limited number of X-ray reflections on which their final three-dimensional refinement was based, and also point out that for A amylose the apparent positions of the water molecules are even less clear-cut (1978*b*).

French (1984) has, therefore, raised the question as to whether the 'A' and 'B' X-ray diffraction patterns obtained from native starch granules and amylodextrins do, in fact, reflect precisely the same crystal structures as in the A and B amylose fibres, and it was to investigate this question further that the work described in this paper was carried out.

In the light of the above discussion it was decided to examine in more detail the similarities between the X-ray powder diffraction patterns obtained from native starch granules and patterns calculated on the basis of the Wu & Sarko models for A and B amylose fibres. The effects on the simulated patterns of a number of simple variations to the 'model' structure, which may have relevance to the starch granule architecture, were investigated. Those considered were:

(i) The effect of variations in the packing 'sense' of the amylose double helices;
(ii) the positions of the water molecules;
(iii) in view of the likely involvement of amylopectin in the crystalline region of the granule, and the evidence in support of a 'racemose' structure (Fig. 2) (French, 1972; Robin *et al.*, 1974), it was also decided to investigate the effect of 'staggering' the double helices on the simulated diffraction patterns;
(iv) the possible effect of the paracrystalline nature of the granule on the diffraction pattern has also been considered in qualitative terms.

Some preliminary measurements of the neutron powder diffraction patterns of B starch in H_2O and D_2O have also been made, and the similarities between these patterns and those calculated from the Wu and Sarko models considered.

MATERIALS AND METHODS

Samples of wheat ('A' type) and potato ('B' type) starch granules were kindly supplied by Drs P. Hart and D. Bates. In both cases the method of extraction was a slightly modified version of that of Adkins & Greenwood (1966). A solution of 0·01 M mercuric chloride was used to inhibit enzymic activity, and residual surface protein was removed by prolonged shaking of the granules in an aqueous suspension of 1

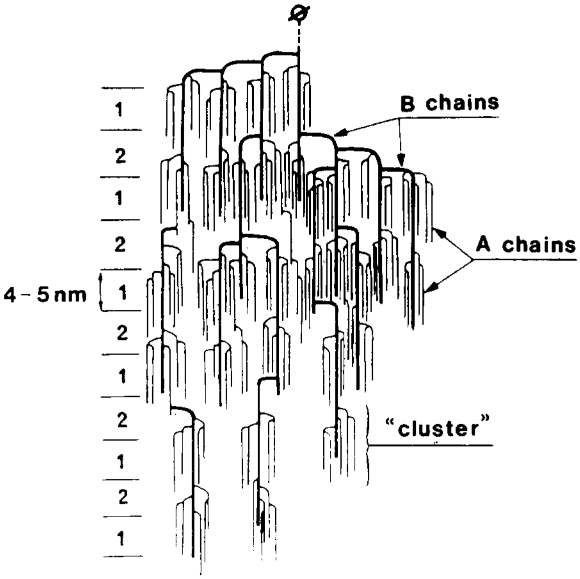

Fig. 2. The racemose model of amylopectin. From Guilbot & Mercier (1985). Reproduced with permission.

volume toluene to 8 volumes saline (specific gravity 1·07407). The starch granules were then air dried (Hart, 1983).

Experimental X-ray powder diffraction patterns for A and B type starches were obtained from a Phillips APD15 automatic powder diffractometer, equipped with a PW1050 vertical goniometer, a Panmure curved graphite crystal monochromator and a scintillation counter. Diffraction patterns were obtained in the symmetrical reflection mode with copper Kα radiation ($\lambda = 0{\cdot}1542$ nm) and with an angular step scan rate of 2 s per 0·05° step.

A check for preferred orientation in the samples was made, using a Laue camera in transmission mode and a flat plate film cassette.

Preliminary measurements of the neutron powder diffraction patterns of B starch in H_2O and D_2O were obtained from the D16 diffractometer at the Institut Laue-Langevin, Grenoble, France. Details of the apparatus have been published elsewhere (Zaccai & Gilmore, 1979; ILL, 1983). Samples of B starch were prepared as slurries in H_2O and 100% D_2O after vacuum-drying in a desiccator. To ensure that H_2O/D_2O exchange had occurred, excess D_2O was decanted from that sample after standing for 1 h and the sample centrifuged before adding more D_2O. This process was repeated several times. The final slurries were placed in 2 mm quartz cells with an excess of solvent and sealed with parafilm. Data were collected, with a neutron wavelength of 0·452 nm in ω, 2θ scans and three measurements were made, with 5 h exposure for the H_2O and 100% D_2O slurries and 3 h exposure for an empty quartz cell, to determine the background scattering. Because of the configuration of the instrument and sample changer, and the limited exposure time available, it was only possible to measure the powder diffraction pattern to a maximum 2θ value of 50°.

Simulated wide-angle X-ray and neutron powder diffraction patterns were calculated, using a modified version of the profile refinement program described by Rietveld (1969), without carrying out refinement. The program assumed the diffraction pattern to be the sum of a number of Gaussian-shaped reflections centred on their respective Bragg angle positions. The contribution Y_i of a Bragg reflection at position $2\theta_i$ to the measured profile intensity is

$$Y_i = (tF_k^2 j_k L_k^2 . 2)(\ln 2)^{1/2}/H_k \pi^{1/2}) \exp[(-4 \ln 2/H_k^2)(2\theta_i - 2\theta_k)^2]$$

where F_k is the structure factor amplitude for Bragg reflection k (X-ray or neutron), t is the step width of the counter, j_k is the multiplicity of the reflection, L_k is the Lorentz factor, $2\theta_k$ is the calculated position of the Bragg peak, corrected for any zero error in the counter and H_k is the full-width at half-height of the Bragg reflection k (Rietveld, 1969). H_k was calculated from the expression

$$H_k^2 = U \tan^2 \theta_k + V \tan \theta_k + W$$

The parameters U, V W were determined empirically by calculating the peak half-width at various Bragg angles, θ, according to the Scherrer expression

$$B = \frac{K\lambda}{L \cos \theta}$$

(Klug & Alexander, 1974, p. 656) and by assuming a crystallite size, L, of 11·0 nm and the value of the constant K to be 0·94. This value of the crystallite size was obtained from a measurement of the half-width of the (100) reflection at approximately 5·5° (2θ) on an experimental B starch diffractogram. The X-ray scattering factors used were those published in the *International Tables for X-ray Crystallography*, Vol. 3 (International Union of Crystallography, Birmingham, Kynoch Press, 1968). A Debye–Waller temperature factor of 7·0 was applied uniformly to the calculated structure factors; no attempt was made to consider the implications of possible differences in the temperature factor for different atoms.

The profile simulation program was validated by generating an X-ray powder diffraction pattern for α-quartz, and experimental and simulated patterns are shown in Fig. 3.

Theoretical powder diffraction profiles for A and B amylose were calculated using the atomic coordinates published by Wu & Sarko (1978*a*,*b*), for the antiparallel-packed helical models. The coordinates of all the atoms in the unit cell (12 glucose residues + water molecules) were generated, and multiplicities for space group P1 used. For the calculation of the neutron powder diffraction patterns in D_2O, the hydrogen atoms of the water molecules and the labile hydrogens of the glucan hydroxyls were replaced by deuterium in the model.

RESULTS

The simulated X-ray powder diffraction profiles for A and B amylose are compared with the experimental patterns from A and B type starches in Fig. 4, with the intensities scaled to the same maximum value. Although the main features of the experimental patterns appear to be reproduced, particularly at low resolution, some important differences remain. In both the A and B type starch patterns a large amount of background scatter is present, due to the amorphous component of the granule. A small difference in unit cell dimensions is also apparent. The simulated patterns were calculated using the unit cell dimensions determined by Wu & Sarko (for A amylose $a = 1{\cdot}152$ nm, $b = 1{\cdot}770$ nm and $c = 1{\cdot}052$ nm; for B amylose $a = b = 1{\cdot}85$ nm, $c = 1{\cdot}04$ nm). A measurement of the position of the (100) Bragg peak (at approximately $2\theta = 5{\cdot}5°$) in the B starch pattern (the only non-overlapping reflection) yields a value for $a = b = 1{\cdot}82$ nm. Similar differences were observed by Buleon *et al.* (1984) in their electron diffraction studies of B amylose crystals (with $a = b = 1{\cdot}8$ nm), and

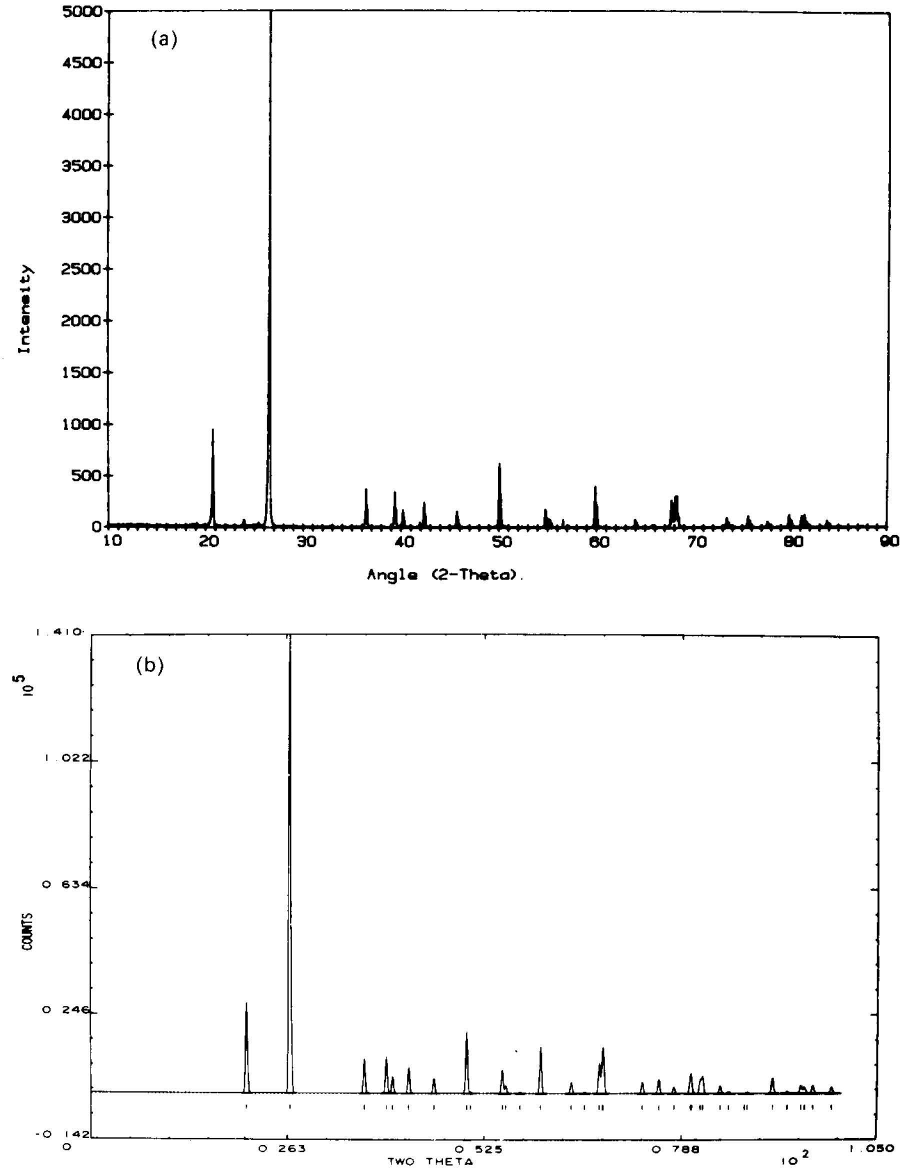

Fig. 3. A comparison of (a) an experimentally determined wide-angle X-ray powder diffraction pattern of α-quartz and (b) the simulated pattern.

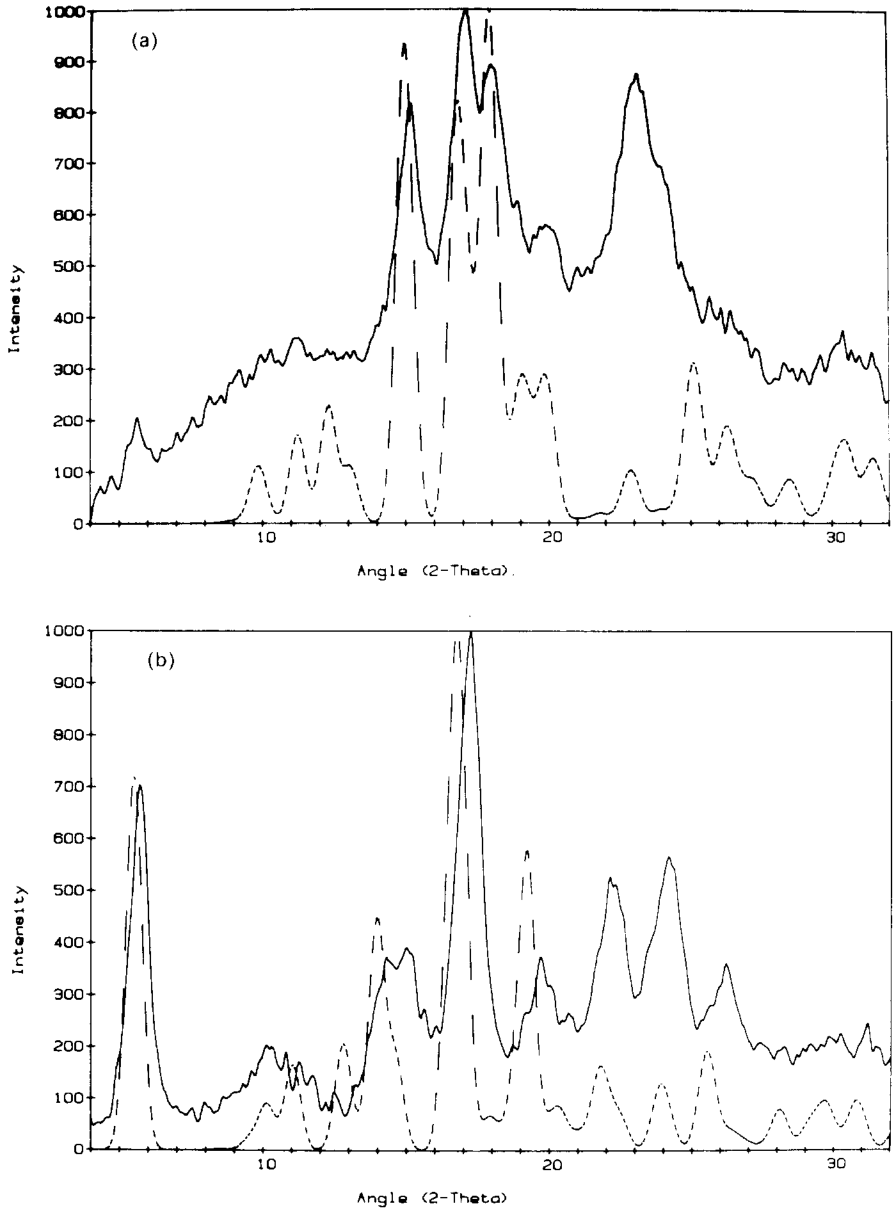

Fig. 4. A comparison of the experimental X-ray powder patterns of (a) A type and (b) B type starch granules (full lines), with the simulated patterns of A and B amyloses (dotted lines).

they interpreted this as probably being due to the fact that their crystals were not fully hydrated.

To simulate the amorphous background, a 'background' profile was prepared by subtracting Gaussian profiles (with appropriate half-widths and intensities) for the most prominent peaks from an experimental starch diffraction pattern. The resulting 'background' profile was then added to the simulated profile to produce the curve shown in Fig. 5(b) for B amylose (calculated with unit cell dimensions $a = b = 1{\cdot}82$ nm and $c = 1{\cdot}042$ nm). Evident differences between the experimental and simulated patterns occur above 17° (2θ)(0·52 nm *d*-spacing), with the peak at 19° appearing much stronger on the simulated pattern than on the experimental one. Figure 5(a) compares an experimental A type starch pattern with the simulated pattern for A amylose (with an added amorphous background). Again, the differences between the patterns are greatest for 2θ angles above 18° (0·49 nm *d*-spacing) with a large discrepancy in the amplitudes of the peaks at $2\theta = 23°$ and 25° (0·36–0·39 nm *d*-spacing).

Since Wu & Sarko (1978*a*) did not publish the coordinates of the 'second best' version of their model with parallel-packed helices, to investigate the effect of parallel as opposed to anti-parallel packing of the amylose double helices a simple parallel packed model was constructed by shifting the helix centred at ($2/3a$, $1/3b$) to the position of the second helix ($1/3a$, $2/3b$). The simulated profiles of A and B amylose with 'parallel' packing (and added amorphous backgrounds) are compared to the experimental A and B starch patterns in Fig. 6. There appear to be fewer differences between the simulated patterns produced by parallel and anti-parallel packing than between the simulated amylose and experimental starch diffraction patterns. The sensitivity of the simulated patterns to the relative positions of the double helices along the *c*-axis of the unit cell was investigated by translating one helix relative to the other in steps of $0{\cdot}25c$. Figure 7 compares the simulated patterns for both A and B amylose with one helix translated relative to the other along *c* by $0{\cdot}75c$ with the experimental granule diffraction patterns. Whilst some differences in intensity are apparent, the main features of the simulated patterns again remain unchanged.

Several authors (Cleven *et al.*, 1978; Wu & Sarko, 1978*a*,*b*; Bluhm *et al.*, 1980) have argued that water molecules play an important role in maintaining the crystal structures of amylose and B starch, and so it was decided to investigate the sensitivity of the simulated patterns for

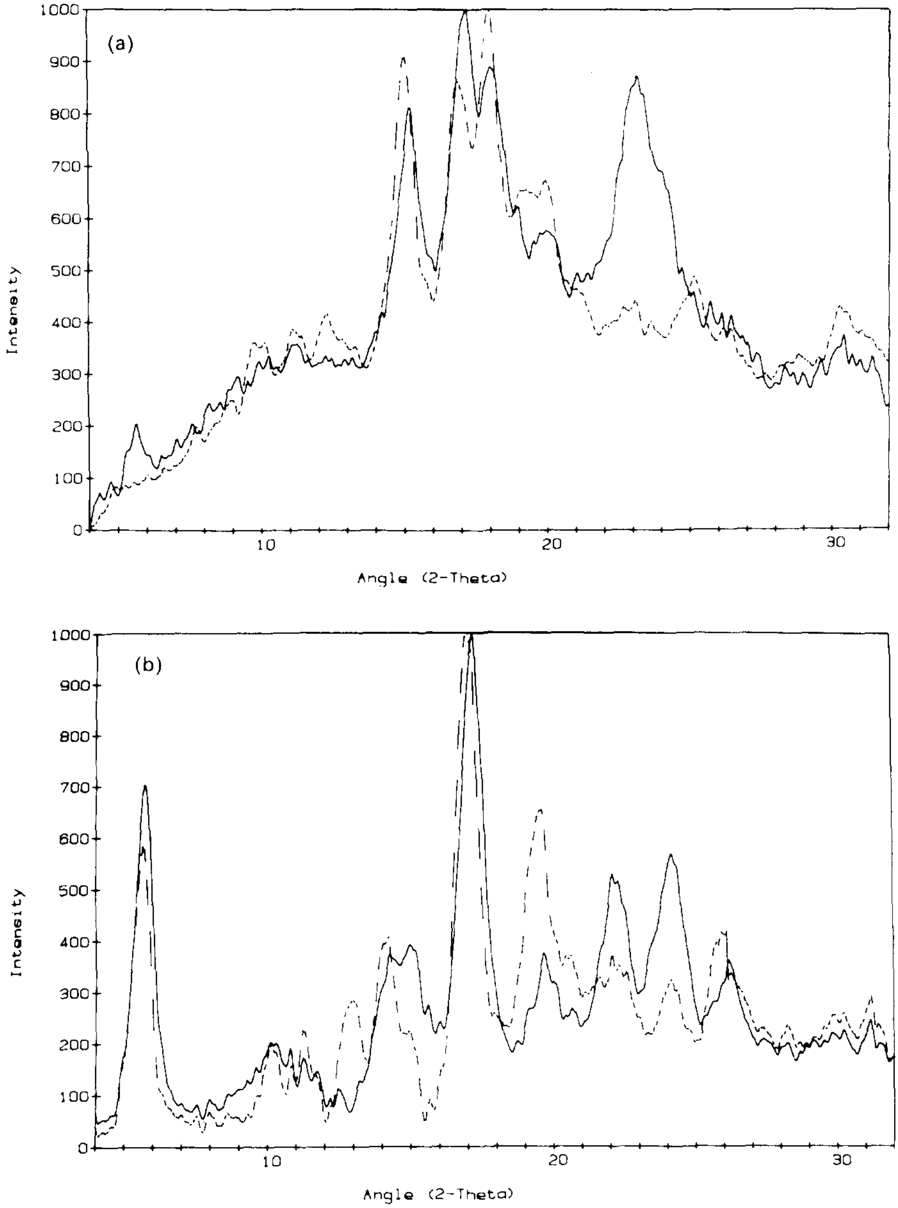

Fig. 5. A comparison of the experimental X-ray powder patterns of (a) A type and (b) B type starch granules (full lines), with the simulated patterns shown in Fig. 4 after addition of an amorphous background (dotted lines).

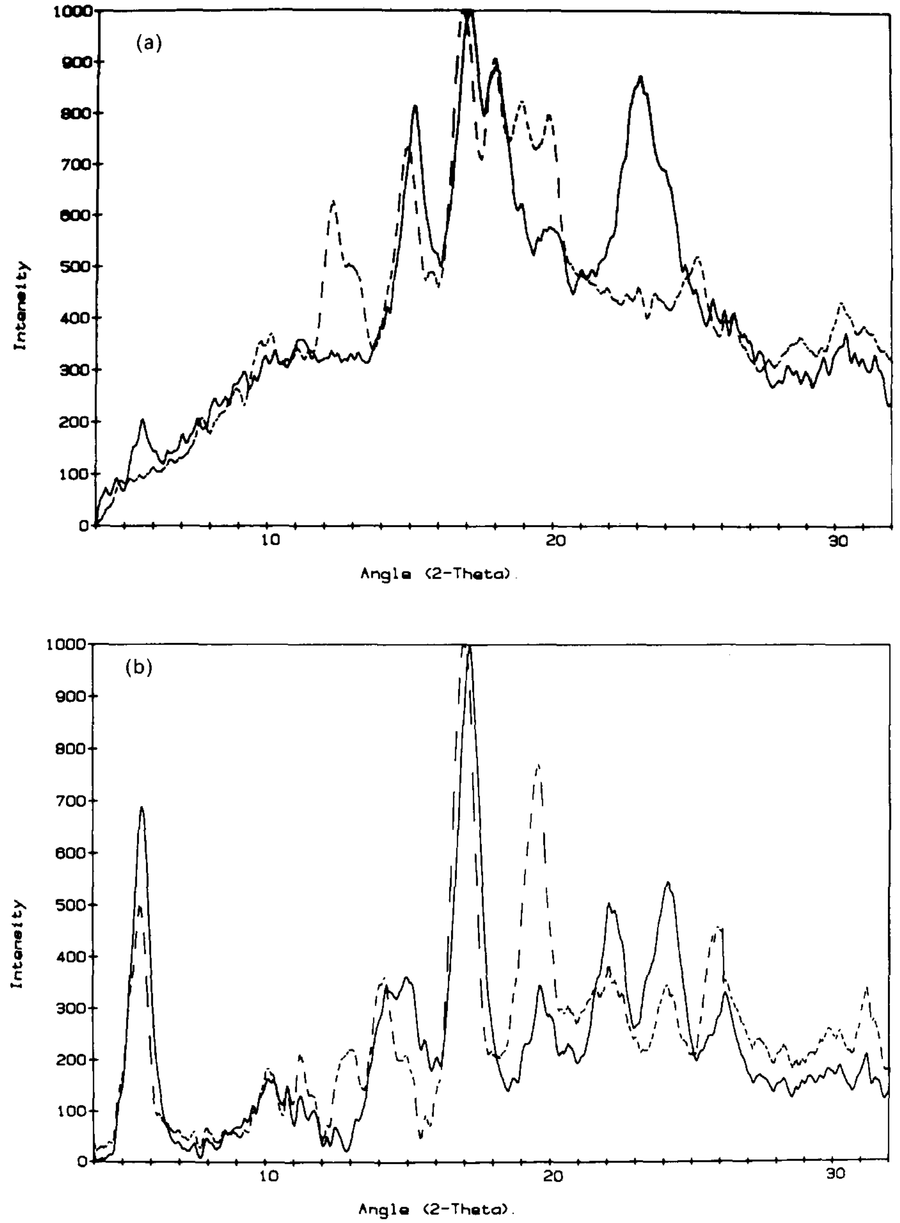

Fig. 6. A comparison of the experimental X-ray powder patterns of (a) A type and (b) B type starch granules (full lines), with the simulated profiles of A and B amyloses calculated from a model with parallel packing (dotted lines).

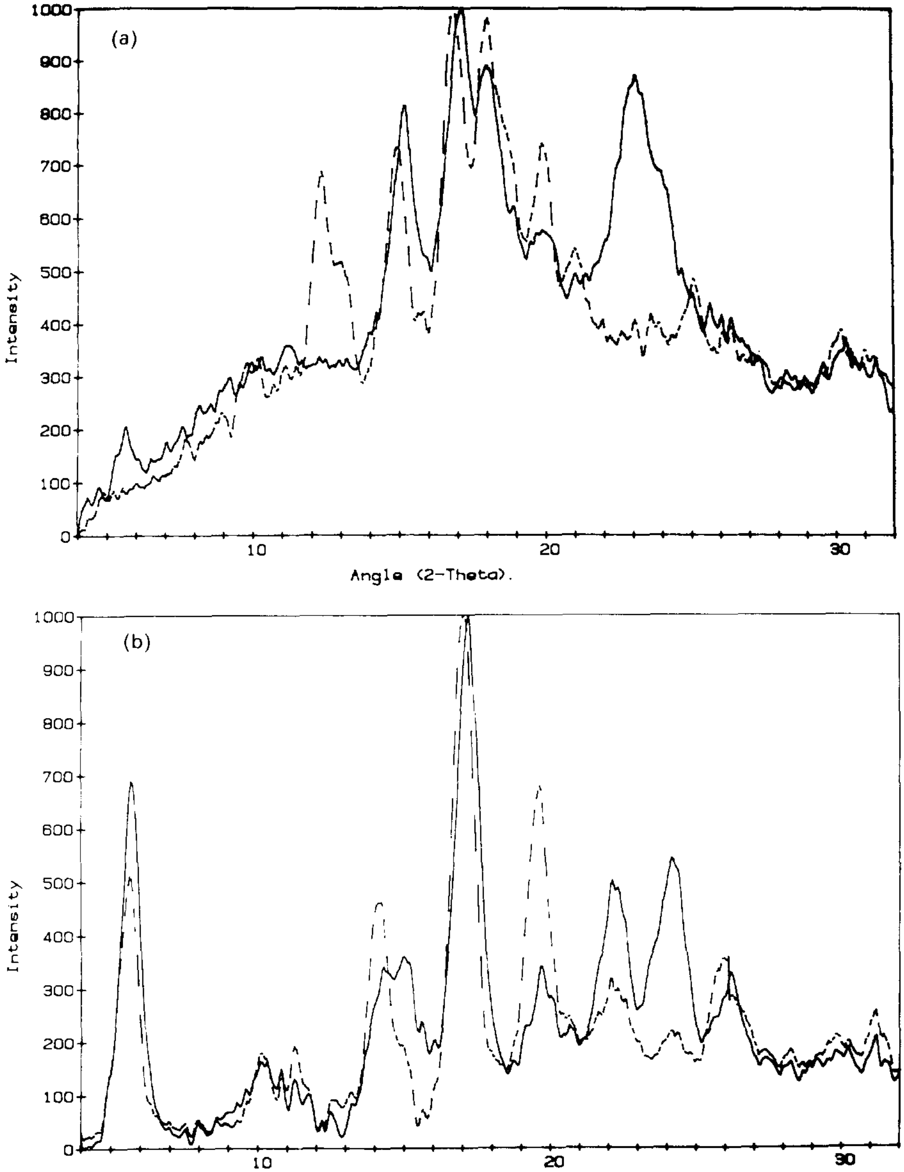

Fig. 7. A comparison of the experimental X-ray powder patterns of (a) A type and (b) B type starch granules (full lines), with the simulated profiles of A and B amyloses calculated from a model with one helix translated relative to the other by 0·75*c* (dotted lines).

B amylose to the positions of the water molecules. Wu & Sarko (1978*a*) began their refinement of the water positions by putting the water molecules into the model in six planes, each containing six water molecules equally spaced around a circle of 0·3 nm radius. The simulated diffraction pattern produced by the anti-parallel packed model containing the 36 water molecules in these symmetrically distributed positions is compared in Fig. 8 with the pattern produced by the same model with the water molecules placed at their final refined positions (coordinates from A. Sarko (pers. comm.)). A number of differences are apparent, particularly in the peaks at 13°, 14°, 19°, 22° and 25·5° (2θ).

Figure 9 shows the simulated wide-angle neutron diffraction patterns for B amylose (anti-parallel packing), with (a) hydrogen atoms and (b) with the water molecules and labile hydrogens of the glucan hydroxyl groups replaced by D_2O and deuterium, respectively. Differences are evident between the patterns in D_2O and H_2O. Some small

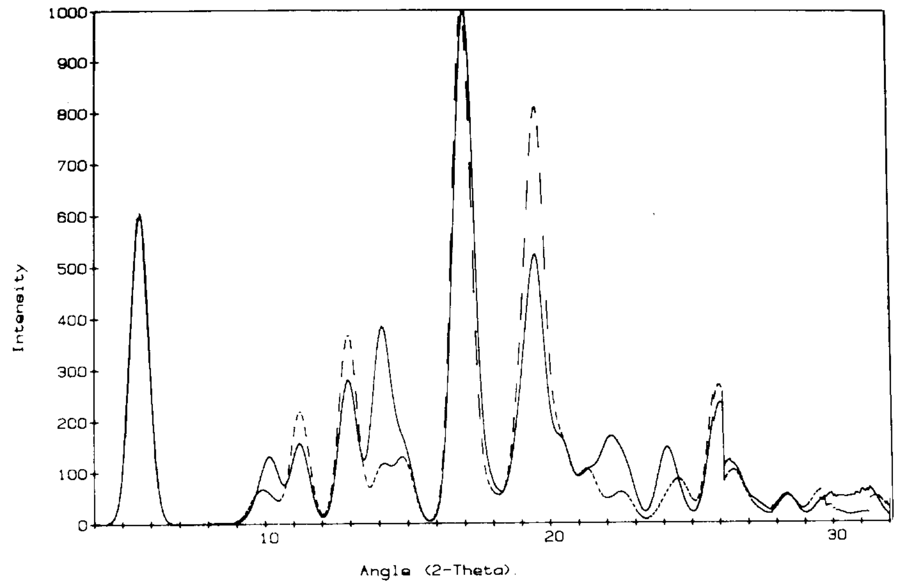

Fig. 8. A comparison of the simulated X-ray powder patterns of B amylose, calculated from (a) the refined model of Wu & Sarko (full lines) and (b) the model with water molecules symmetrically distributed about the origin (dotted lines).

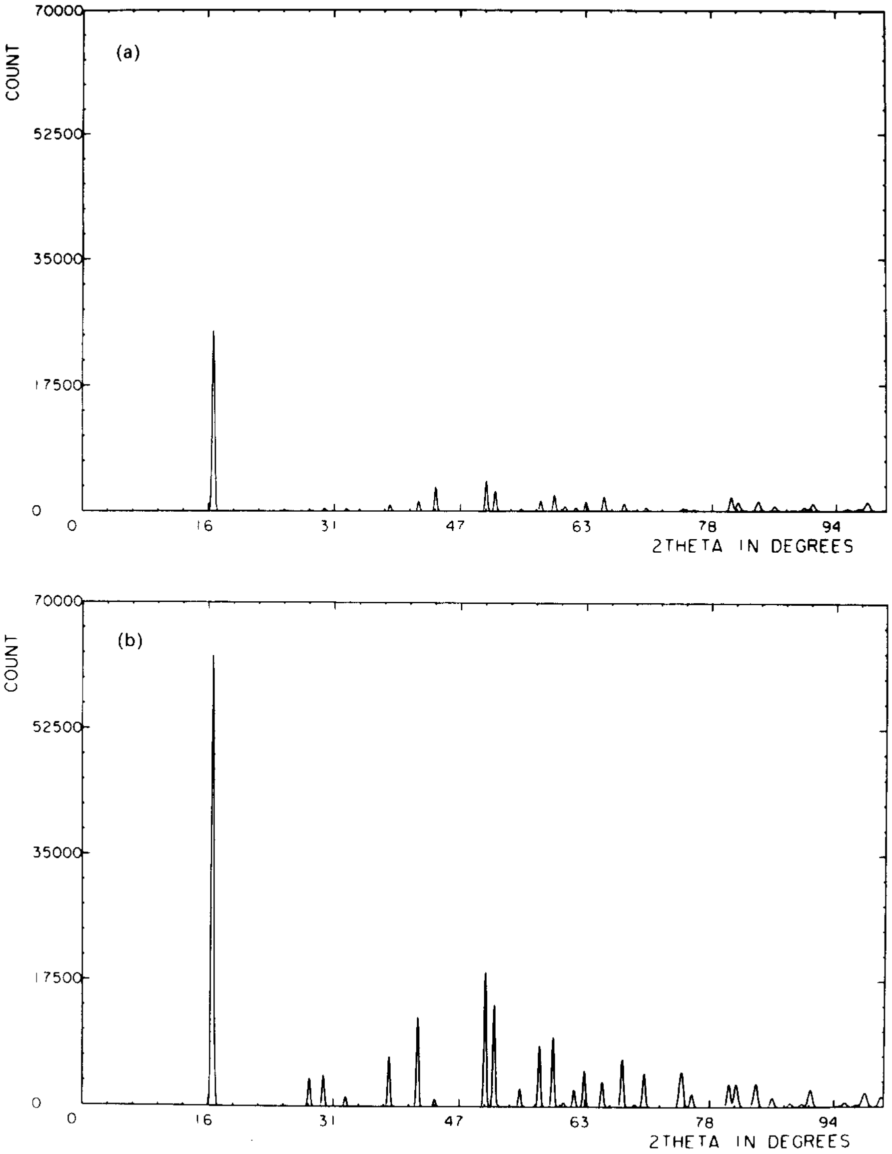

Fig. 9. The simulated wide-angle neutron powder diffraction patterns of B amylose (anti-parallel packing) with (a) water molecules and (b) water molecules and labile glucan hydroxyl hydrogen atoms replaced by D_2O and deuterium respectively.

changes are also apparent between the calculated patterns in H_2O and D_2O of the parallel (Fig. 10(a), (b)) and anti-parallel packed models. Figure 11 shows the experimental powder diffraction patterns obtained from the sample of B starch in (A) H_2O and (B) D_2O (and (C) the scattering from an empty quartz cell) to a maximum 2θ value of 50°. The most prominent peaks in the D_2O pattern correspond to the expected positions of the (100) and (110) reflections (*d*-spacings of 1·612 and 0·92 nm, respectively). In the H_2O sample only the (100) reflection is observable, as predicted by the simulated diffraction patterns (Fig. 9), in which the (110) reflection appears extremely weak in the H_2O pattern. The other apparent small 'peaks' in the experimental patterns do not appear at positions which correspond to Bragg peaks in the simulated patterns and were not considered to be significant, although better counting statistics would obviously be necessary to confirm this. An amorphous background peak can be observed in the H_2O sample (Fig. 11(a)), but is absent in the D_2O sample (Fig. 11(b)).

DISCUSSION

Although the main features of the experimental X-ray powder diffraction patterns of A and B starch appear in the simulated patterns based on the crystal structures of A and B amylose, the above results also indicate a number of discrepancies. Preferred orientation appears to be ruled out as an explanation of these differences, since the flat plate photographs of the starch powder samples did not indicate the presence of any significant preferred orientation.

Although a number of possible variations to the model structure which may have relevance to the granule architecture were explored, none of these have explained the discrepancies observed between the experimental and simulated patterns. The main features of the simulated profiles appear to be determined by the two 'cylinders' of carbohydrate molecules positioned at the appropriate points in the unit cell. As long as the appropriate crystal packing was maintained, small variations in the actual atomic positions within these cylinders did not alter the simulated profiles to any large extent. Thus inversion of one of the helices (to produce parallel packing) or translation of one cylinder relative to the other in the *c* direction of the unit cell ('stagger-

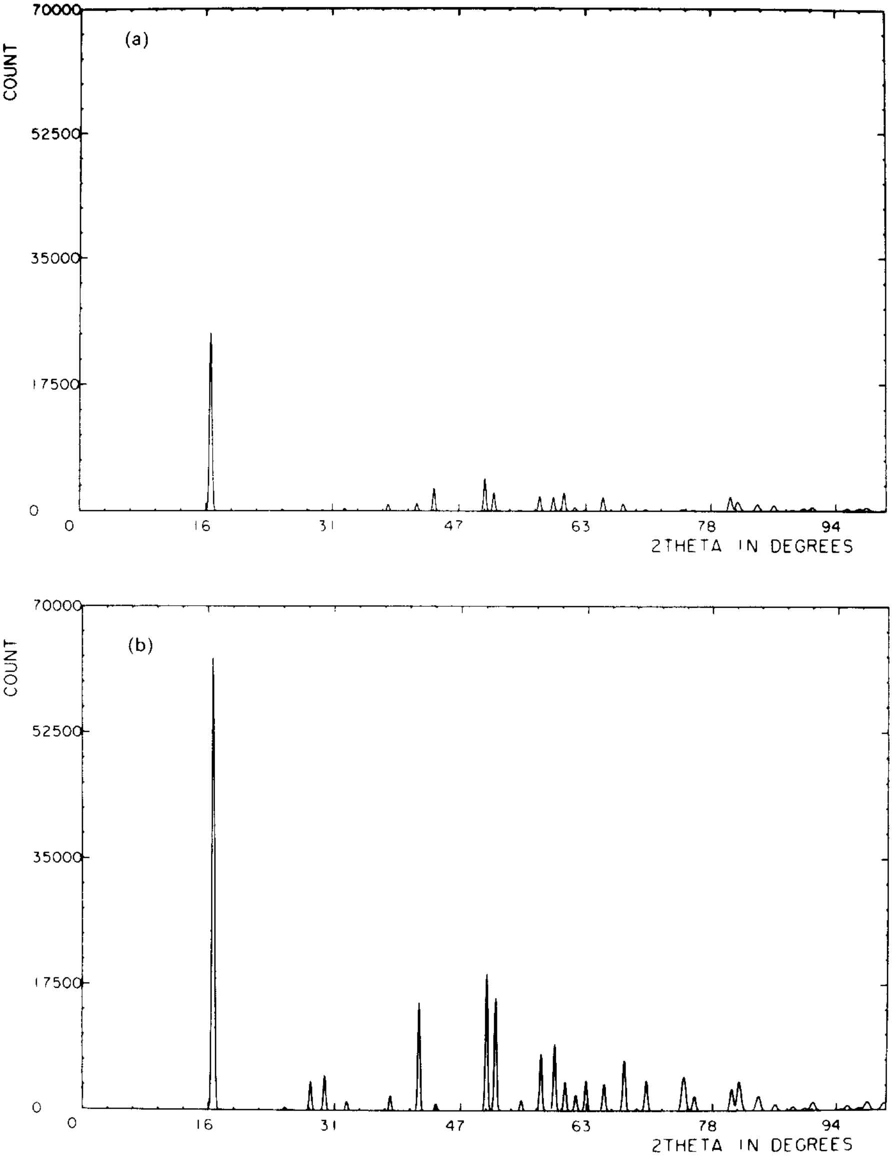

Fig. 10. The simulated wide-angle neutron powder diffraction patterns of B amylose (parallel packing) with (a) water molecules and (b) water molecules and labile glucan hydroxyl hydrogen atoms replaced by D_2O and deuterium, respectively.

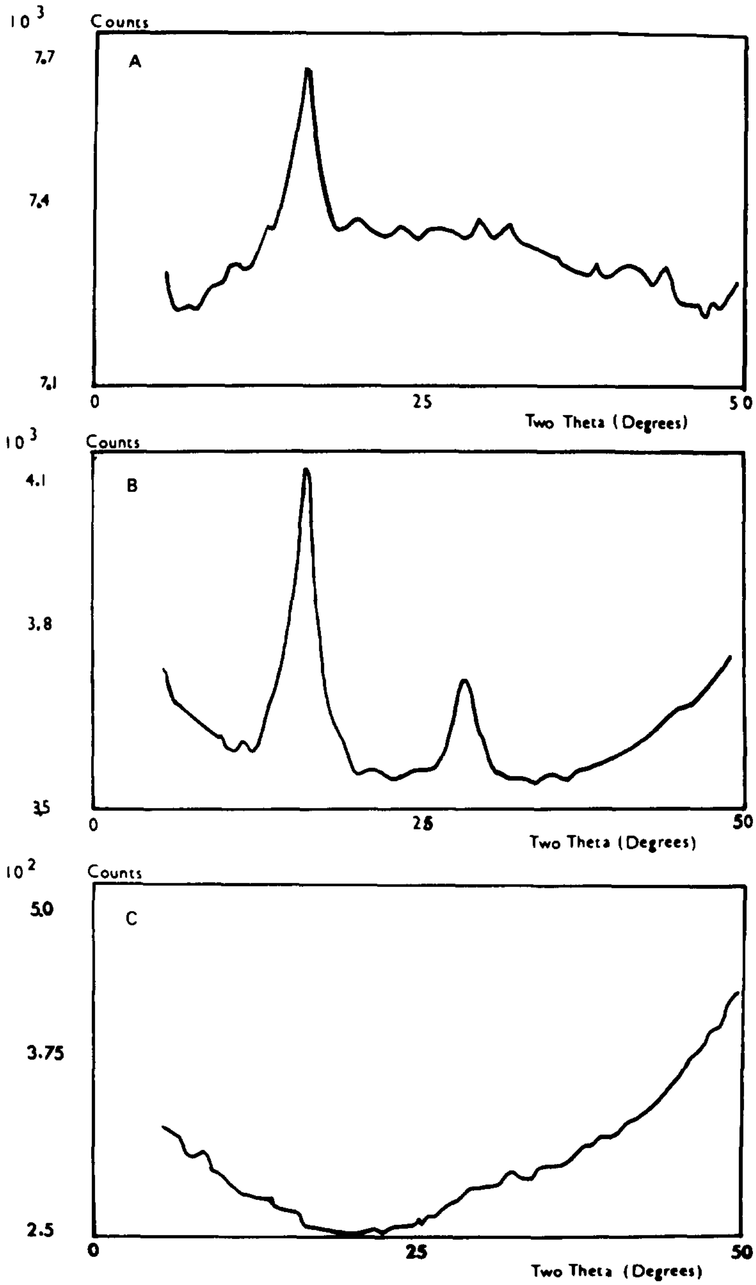

Fig. 11. Experimental neutron powder diffraction patterns from B type starch granules in (A) H_2O and (B) D_2O. The scattering from an empty quartz cell is shown in (C).

ing') did not produce remarkably large variations in the simulated profiles. The discrepancies between the profiles produced by these models and the experimental profiles were just as great as those between the experimental profiles and the profiles produced by the original model of Wu & Sarko (1978*a*,*b*). It has thus not been possible, on the basis of this technique, to make any distinction between parallel and anti-parallel packed models, or between models in which the double helical amylose cylinders were in-step or staggered.

Several authors have argued that water molecules play an important role in the crystalline organization of B amylose and B starch (Sterling, 1960; Guilbot *et al.*, 1961; Kainuma & French, 1972). Kainuma & French (1972) suggested that water may act as a kind of 'plasticizer', promoting an alignment of the starch molecules into a highly ordered crystalline array. Cleven *et al.* (1978) observed that the positions of the diffraction maxima for B starch shifted towards greater lattice plane spacings with increasing hydration of the sample. The intensities of the peaks at approximately 5·5° and 25·5° (2θ) also showed marked increases in intensity with increasing hydration. Cleven *et al.* interpreted the changes in the 25·5° peak (corresponding to an interplanar spacing of 0·37 nm) as arising from the development of an ordered water structure in which the water molecules are structured like cubic ice. Duprat *et al.* (1980) have also observed an increase in the 5·5° peak and an increase in the volume of starch granules during hydration. They interpret their results in terms of an expansion in the intercrystalline amorphous phase, forcing the crystallites to become aligned.

From Fig. 8 it can be seen that the relative intensities of many of the peaks in the simulated patterns do appear to be sensitive to the precise locations of the water molecules. The peak at approximately 5·5° (2θ) in the B starch diffraction pattern represents the (100) reflection and is the only non-overlapping reflection present. Water molecules distributed about the origin of the unit cell, as in the model of Wu & Sarko, would be expected to contribute to the structure factor amplitude for this reflection, and the observation that the (100) reflection is sensitive to water content would appear to be consistent with this distribution of water molecules. However, the water structure of the granule is unlikely to be modelled precisely by the fixed atomic coordinates for the water molecules used in the simulations, and disorder in the water structure is one possible factor contributing to the differences between the simulated and observed diffraction profiles.

The preliminary results obtained from neutron diffraction of B starch are also of interest in considering the positions of the water molecules. Since there is a large difference between the coherent neutron scattering lengths for hydrogen and deuterium $-0{\cdot}3742$ and $0{\cdot}6671 \times 10^{-12}$ cm, respectively), neutron diffraction patterns obtained from samples in H_2O and D_2O could yield information about the areas in which H/D exchange has taken place, including areas of hydration (Jacrot, 1976; Zaccai & Gilmore, 1979). The very limited neutron diffraction profiles measured for B starch appear to be consistent with the calculated profiles based on the Wu & Sarko model, i.e. the (110) reflection is observable in the D_2O pattern, but not in the H_2O pattern. This would tend to support the general distribution of water molecules in the Wu & Sarko model, in a central channel in a hexagon of amylose double helices. However, these data are preliminary, and it would be necessary to measure the neutron powder diffraction pattern to very much higher resolution to confirm, with any degree of certainty, the areas of hydration, preferably by the use of Difference Fourier techniques (Zaccai & Gilmore, 1979). The observation that an amorphous background 'peak' is present in the H_2O sample, but appears to be 'contrast-matched' out in the D_2O sample, suggests that part of the amorphous component of the granule may also consist of water (or exchangeable hydrogen atoms).

Disorder in the granule structure remains as another possible explanation for the differences observed between the experimental and simulated patterns. As Kakudo & Kasai (1972, p. 146) point out, crystals of synthetic high polymers are likely to be inherently defective if the molecules are of different lengths. The variable lengths of the amylose and amylopectin molecules comprising the granule will probably contribute to such a disordered structure. Chemical and physical evidence suggests that the structure of many high polymer solids consists of various regions with different degrees of internal order, ranging from almost perfectly crystalline to completely amorphous (Kakudo & Kasai, 1972, p. 111). The intermediate state of paracrystallinity has been decribed by Hosemann (Hosemann, 1950; Hosemann & Bagchi, 1962), who divided crystal lattice distortions into two categories: distortions of the 'first kind', in which long-range order is preserved but atoms are displaced from their ideal lattice point positions; and distortions of the 'second kind', in which long-range order is lost and each lattice point varies in relation to its nearest neighbours. It is distortions of the second type which are responsible for the phenomenon of paracrystallinity (Alexander, 1969, pp. 426–7; Kakudo & Kasai, 1972, pp. 113–14). The effect of distortions of the second kind on the X-ray diffraction profile is a reduction in profile intensity and an increase in diffuseness with Bragg angle 2θ (or reflection order, m) (Alexander, 1969, p. 426; Kakudo & Kasai, 1972, p. 30). This broadening also increases with increasing lattice distortion. The experimental diffraction patterns of the granules exhibit the qualitative characteristics of paracrystalline materials. In theory, it should be possible to separate crystallite size and lattice distortion factors for a paracrystalline specimen if the intensities of several orders of reflections from a given family of planes can be measured. Hosemann (Hosemann, 1950; Hosemann & Bagchi, 1962) defines a lattice distortion factor, for distortions of the second kind, $g_{\mathrm{II}}=(\Delta d_{\mathrm{II}})/\bar{d}$, which describes the relative distribution fluctuation of the lattice vector perpendicular to a set of planes. The expression for reflection breadth obtained from the Scherrer equation must then be replaced by

$$\begin{aligned}\beta_{hkl}^{2} &= \beta_{c}^{2}+\beta_{\mathrm{II}}^{2}\\ &= \frac{1}{\bar{L}_{hkl}^{2}}+\frac{\pi^{4} g_{\mathrm{II}}^{4} m^{4}}{d_{hkl}^{2}}\end{aligned}$$

where β_c and β_{II} are the integral reflection breadths due to crystallite size and lattice distortions of the second kind, respectively, $\bar{L}$ is the mean crystallite size perpendicular to the planes, m is the order of reflection (hkl) and d_{hkl} is the interplanar spacing (Hosemann, 1950; Hosemann & Bagchi, 1962; Alexander, 1969, p. 429).

Thus, provided that at least two orders of diffraction from planes (hkl) can be resolved g_{II} can be determined from a plot of β^2 against m^4 (Alexander, 1969, p. 429). Unfortunately, it was not possible to carry out this analysis here, since there is only one distinctly resolved peak in the experimental diffraction profiles, the (100) reflection at approximately 5·5° (2θ).

CONCLUSIONS

The main features at low resolution of the X-ray powder diffraction patterns of A and B starch granules appear to be reproduced in simulated profiles calculated on the basis of the Wu & Sarko structures of A and B amyloses. However, several discrepancies between the observed and calculated patterns are evident at higher resolution, and these do not appear to be simply due to the packing sense of the amylose double helices in the unit cell.

The X-ray powder diffraction patterns of starch granules appear to show the qualitative characteristics of those of paracrystalline materials, and disorder in the granule structure could be a factor contributing to the discrepancies between the observed diffraction patterns and those calculated on the basis of the crystal structures of A and B amylose.

The preliminary neutron diffraction data obtained from B type starch granules appear to be consistent with the general position of water molecules in the crystal structure of B amylose, i.e. with the water molecules situated in a channel in the centre of a hexagon of amylose double helices. However, many peaks in the simulated diffraction profiles do appear to be sensitive to the positions of water molecules in the model, and disorder in the water structure of the granule may also be a factor contributing to the differences between the observed and simulated profiles.

Further work would be necessary to confirm this, and also to clarify the contribution of paracrystallinity to the overall X-ray diffraction profiles of starch granules.

ACKNOWLEDGEMENTS

The authors wish to record their grateful thanks to the Agricultural and Food Research Council for financial support for D.L.W.; to the Neutron Division of the Rutherford Appleton Laboratory for the Rietveld refinement program; to Dr G. Zaccai (Institut Laue-Langevin) for help with the collection of neutron diffraction data and subsequent discussions; to Mr W. B. Roys (Nottingham University Physics Department) for the use of a flat plate X-ray camera; and to Dr D. Brown (Loughborough University) and Dr N. J. Begley (Nottingham University) for useful discussions. We also wish to thank Drs R. D. L. Marsh, D. Bates and S. Wynne-Jones (Nottingham University Food Science Laboratories) for their valuable collaboration, and Dr A. Fitch (Institut Laue-Langevin) for help with the preparation of some of the figures.

REFERENCES

Adkins, G. K. & Greenwood, C. T. (1966). *Stärke* **18**, 213.

Alexander, L. E. (1969). *X-ray diffraction methods in polymer science*, New York, John Wiley.

Bluhm, T., Deslandes, Y., Marchessault, R. H. & Sundararajan, P. R. (1980). *ACS Symp. Series 127*, Washington, DC, American Chemical Society, p. 253.

Brant, D. A. (1976). *Q. Rev. Biophys.* **9** (4), 527.

Buleon, A., Duprat, F., Booy, F. P. & Chanzy, H. (1984). *Carbohydr. Polym.*, **4**, 161.

Charbonnière, R., Mercier, C., Tollier, M. T. & Guilbot, A. (1968). *Stärke* **20**, 75.

Cleven, R., van den Berg, C. & van der Plas, L. (1978). *Stärke* **30**, 223.

Duprat, F., Gallant, D., Guilbot, A., Mercier, C. & Robin, J. P. (1980). In *Les polymères végétaux*, ed. B. Monties, Paris, Gauthier-Villars.

French, D. (1972). *J. Jap. Soc. Starch Sci.* **19**, 8.

French, D. (1984). In *Starch, chemistry and technology*, 2nd edn, ed. R. L. Whistler, J. N. Bemiller & E. F. Paschall, London, Academic Press.

Guilbot, A., Charbonnière, R. & Drapron, R. (1961). *Stärke* **13**, 204.

Guilbot, A. & Mercier, C. (1985). Starch. In *The polysaccharides*, Vol. 3, ed. G. O. Aspinall, New York, Academic Press.

Hart, P. (1983). PhD Thesis, Nottingham University.

Hosemann, R. (1950). *Z. Physik.* **128** (1), 464.

Hosemann, R. & Bagchi, S. N. (1962). *Direct analysis of diffraction by matter*, Amsterdam, North Holland.

ILL (1983). *Neutron research facilities at the ILL high flux reactor*, Grenoble, Institut Laue-Langevin.

Jacrot, B. (1976). *Reports in Prog. Phys.* **39**, 915.

Kainuma, K. & French, D. (1972). *Biopolymers* **11**, 2241.

Kakudo, M. & Kasai, N. (1972). *X-ray diffraction by polymers*, Kodansha, Tokyo and Elsevier, Amsterdam.

Katz, J. R. & Van Itallie, T. B. (1930). *Z. Physik. Chem.* **A150**, 90.

Klug, H. P. & Alexander, L. E. (1974). *Xray diffraction procedures for polycrystalline and amorphous materials*, 2nd edn, New York, John Wiley.

Kreger, D. R. (1951). *Biochim. Biophys. Acta* **6**, 406.

Meyer, K. H. (1942). *Adv. in Colloid Sci.* **1**, 183.

Montgomery, E. M. & Senti, F. R. (1958). *J. of Polymer Sci.* **18**, 1.

Rietveld, H. M. (1969). *J. Appl. Cryst.* **2**, 65.

Robin, J. P., Mercier, C., Charbonnière, R. & Guilbot, A. (1974). *Cereal Chem.* **51**, 389.

Sarko, A. & Wu, H. C. (1978). *Stärke* **30**, 73.

Sterling, C. (1960). *Stärke* **12**, 182.

Wu, H. C. & Sarko, A. (1978*a*). *Carbohydr. Res.* **61**, 7.

Wu, H. C. & Sarko, A. (1978*b*). *Carbohydr. Res.* **61**, 27.

Zaccai, G. & Gilmore, D. J. (1979). *J. Mol. Biol.* **132**, 181.